Pergamon

0017-9310(95)00046-1

Correlation of Sauter mean diameter and critical heat flux for spray cooling of small surfaces

KURT A. ESTES and ISSAM MUDAWAR†

Boiling and Two-Phase Flow Laboratory, School of Mechanical Engineering, Purdue University,
West Lafayette, IN 47907, U.S.A.

Abstract—Experiments were performed to understand better nucleate boiling heat transfer and critical heat flux (CHF) for full cone sprays. The effects of spray nozzle, volumetric flux, subcooling and working fluid were investigated. Dense sprays greatly reduced evaporation efficiency, and their boiling curves exhibited an unusually small increase in slope upon transition between the single phase and nucleate boiling regimes. Sauter mean diameter (SMD) data were successfully correlated for fluids with vastly different values of surface tension. This correlation was based upon orifice diameter and the Weber and Reynolds numbers of the orifice flow prior to liquid breakup. Also developed was a new CHF correlation which accurately predicted data for FC-72, FC-87 and water. This correlation shows a strong dependence of CHF on volumetric flux and Sauter mean diameter. It is shown that by combining the correlations for CHF and SMD it is possible to predict accurately CHF for full cone sprays without having to conduct expensive and laborious drop sizing measurements for each individual nozzle.

1. INTRODUCTION

Despite the importance of sprays in many low-temperature, high heat flux situations, little information exists in the literature on the heat transfer mechanisms associated with spray cooling. Investigators have suggested different parametric trends associated with both nucleate boiling and CHF (critical heat flux), but these trends were sometimes contradictory to one another and, to the most part, limited to a particular nozzle and a single working fluid.

Sprays are generally more difficult to characterize than other boiling systems. Heat transfer correlations for jets, for example, can be easily developed using well-defined characteristic lengths (heater size, jet diameter) and characteristic velocity (jet velocity). Choice of scaling parameters for sprays, on the other hand, is complicated by the absence of a coherent fluid flow downstream from the spray nozzle. As liquid breakup takes place, drops are formed which acquire different diameters, velocities, and trajectories, rendering the use of global scaling parameters questionable. In fact, much of the difficulty in using existing heat transfer data for sprays stems from the contradictory recommendations by different investigators concerning which characteristic velocity and characteristic length one should use in correlations. For example, while most studies suggest spray CHF data be correlated with respect to the spray's volumetric flux and drop size [1–4], others recommend reducing the data relative to mean drop velocity and heater size [5].

While one would intuitively attempt to correlate CHF data with respect to drop velocity, it is important to recognize that spray cooling is a commutative effect of many drops impacting the heated surface. Liquid arrives at the surface with a volumetric flux Q'' which equals the volume flow rate striking an infinitesimal portion of the impact area divided by the area of the same portion. Different sprays can possess equal mean drop velocities but with vastly different volumetric fluxes. Failure of drop velocity to account for the commutative effects of multiple drop impact is why drop velocity is not recommended for correlating spray CHF data. In fact, all attempts at correlating the present CHF data with respect to mean drop velocity instead of volumetric flux proved very unsuccessful.

The present study complements the study by Mudawar and Valentine [2] which provided dimensionless spray heat transfer correlations based on water data obtained over a broad range of flow rates and for drastically different spray types, including full cone, hollow cone and flat sprays. CHF data were correlated with respect to the local volumetric flux, Q'', and Sauter mean diameter (SMD), d_{32}.

$$\frac{q''_m}{\rho_g Q'' h_{fg}} = f\left(\frac{\rho_f}{\rho_g}, \frac{\rho_f Q''^2 d_{32}}{\sigma}, \frac{\rho_f c_{p,f} \Delta T_{sub}}{\rho_g h_{fg}}\right). \quad (1)$$

In a comprehensive review of the spray boiling literature [6], it was determined that most studies, including Mudawar and Valentine's, were conducted with only one working fluid, precluding any definitive assessment of the impact of key spray parameters, such as surface tension, on the reported trends. The present study attempts to: (1) develop an under-

---

†Author to whom correspondence should be addressed.

standing of nucleate boiling and CHF in sprays; (2) construct a universal CHF correlation for sprays using newly acquired data for Fluorinerts FC-72 and FC-87 along with the water CHF data obtained earlier by Mudawar and Valentine. While the two Fluorinerts share similar thermophysical properties (except for saturation temperature, 56 °C for FC-72 and 30 °C for FC-87), their surface tension is only about 17% of the surface tension for water. The bulk of the new data was for FC-72 since the low saturation temperature of FC-87 resulted in pump cavitation and magnetic decoupling at high flow rates.

Recently, Estes [6] determined that volumetric flux is a maximum directly beneath the spray nozzle and decays towards the outer edge of the spray impact area. A theoretical model was developed which accurately predicted the volumetric flux distribution across the heated surface. He also demonstrated that CHF for square heaters can be maximized by adjusting the nozzle-to-surface distance such that the spray impact area just inscribes the square surface of the heater. Therefore, all the Fluorinert data presented in the present study were taken with the spray conforming to this optimum configuration.

2. EXPERIMENTAL FACILITY

A two-phase flow loop was assembled which both maintained the desired pressure within the test chamber housing the heater and facilitated precise conditioning of the fluid flow rate and subcooling

upstream of the spray nozzle. The fluid was de-aerated in the same loop prior to each test.

Situated directly below the test chamber was the loop reservoir as shown in Fig. 1. A magnetically coupled centrifugal pump circulated the Fluorinert through the loop which consisted of insulated stainless steel and inert plastic components. Only a small fraction of the total flow delivered by the pump (about 2.52×10^{-3} m^3 s^{-1} (40 gpm)) was actually routed to the nozzle, the balance was bypassed to the reservoir. Two flat plate heat exchangers were employed to remove the heat added to the liquid by the pump. The spray liquid was routed through a carbon filter before being reheated by an in-line electrical heater, and either heated or cooled, as needed, via a third flat plate heat exchanger. Water supplied to this third heat exchanger was circulated through a constant temperature bath; this enabled fine tuning of the spray temperature. One of two rotameters with overlapping flow-rate ranges was used to measure the flow rate prior to entering the nozzle, and the nozzle inlet pressure was measured with the aid of a pressure gauge situated just upstream of the nozzle. After exiting the nozzle and impinging upon the heater surface, the evaporated portion of the flow was condensed within the test chamber and recovered along with the unevaporated liquid through a large diameter drain at the bottom of the test chamber, leading directly to the reservoir.

As shown in Fig. 2(a), the test chamber housed the heater module, spray nozzle assembly and a water-
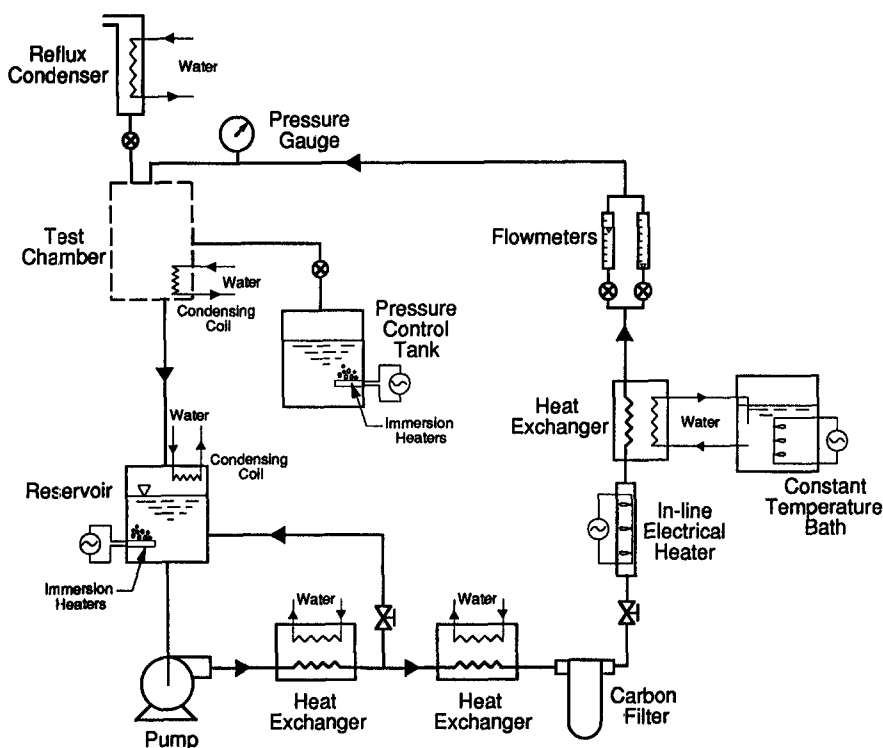
Fig. 1. Schematic of flow loop.

cooled condenser. The heater was machined from oxygen-free copper and was powered by a thick-film electrical resistor silver soldered to its underside. As shown in Fig. 2(b), the heater rested upon a bracket which provided thermal insulation on all surfaces of the heater except the impact surface. Surface temperature was extrapolated from a thermocouple embedded beneath the surface, assuming one-dimensional heat conduction. The surface of the heater was polished prior to each test.

Located along a normal axis centered with respect to the heater surface was a vertical tube to the end of which different spray nozzles could be mounted. The nozzle was raised or lowered to the desired precise placement relative to the heater surface with the aid of a digital micrometer translation stage bolted atop the test chamber.

Uncertainties in the measurement of pressure, flow rate and heater power were estimated at 0.5%, 1.6% and 1% respectively, and thermocouple measurements were made with a ±0.2 °C accuracy. Heat loss to the heater surroundings was determined numerically to be less than 4.5% and 1% during the single-phase and boiling regimes respectively.

3. RESULTS AND DISCUSSION

Three Spraying Systems full cone spray nozzles, designated as nozzles 1, 2 and 3, in order of increasing flow capacity, were used to acquire the FC-72 data.

Table 1 gives the important parameters for the three nozzles.

Spray boiling curves

Boiling curves for FC-72 at 13 °C subcooling are presented in Figs. 3(a)–(c) for nozzles 1, 2 and 3 respectively. At the low volumetric flow rates associated with nozzle 1, a sharp increase in slope seems to mark the commencement of nucleate boiling. However, at the larger flow rates associated with nozzles 2 and 3, this increase in slope is much less discernible. In fact, CHF for both nozzles seems to occur following only a short nucleate boiling heat flux span.

Figures 4(a)–(c) show boiling curves for nozzle 1 at three increasing flow rates that illustrate the effect of subcooling. At the lowest flow rate, the nucleate boiling regime is quite evident at all three subcoolings. However, the nucleate boiling heat flux span gets smaller as subcooling and flow rate increase, becoming virtually non-existent for the highest volumetric flow rate and highest subcooling. Evidently, the span of the nucleate boiling regime is dependent on both subcooling and flow rate, lower subcoolings and flow rates being conducive to a broader nucleate boiling heat flux range.

Figure 5 shows spray boiling curves for water adapted from ref. [2]. These curves clearly depict an increase in both the single-phase heat transfer coefficient and CHF with increasing Q'' or decreasing d_{32}. Also evident in the same figure is the convergence
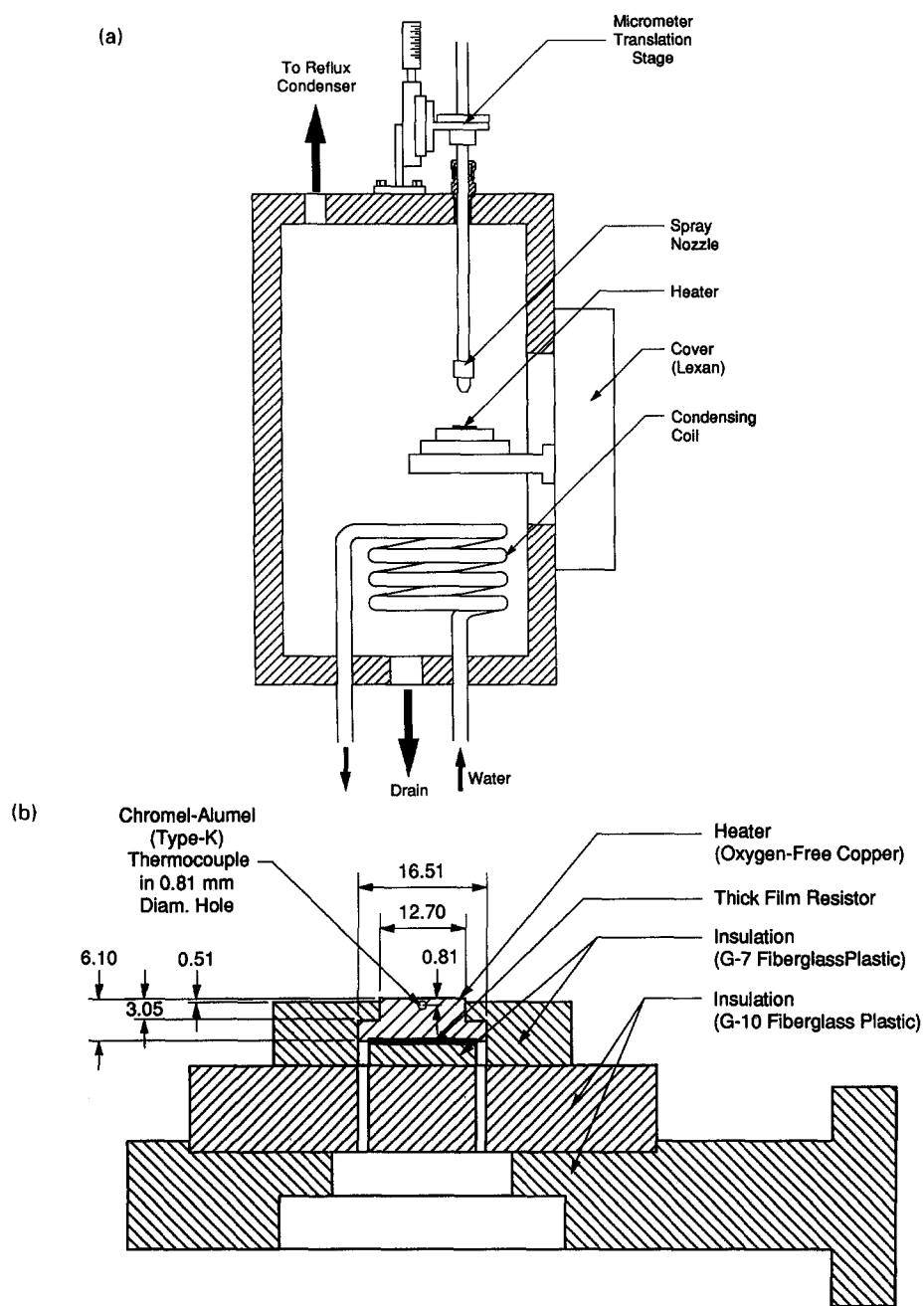
Fig. 2. (a) Schematic of test section and (b) construction of heater module.

Table 1. Characteristics of the spray nozzles using FC-72

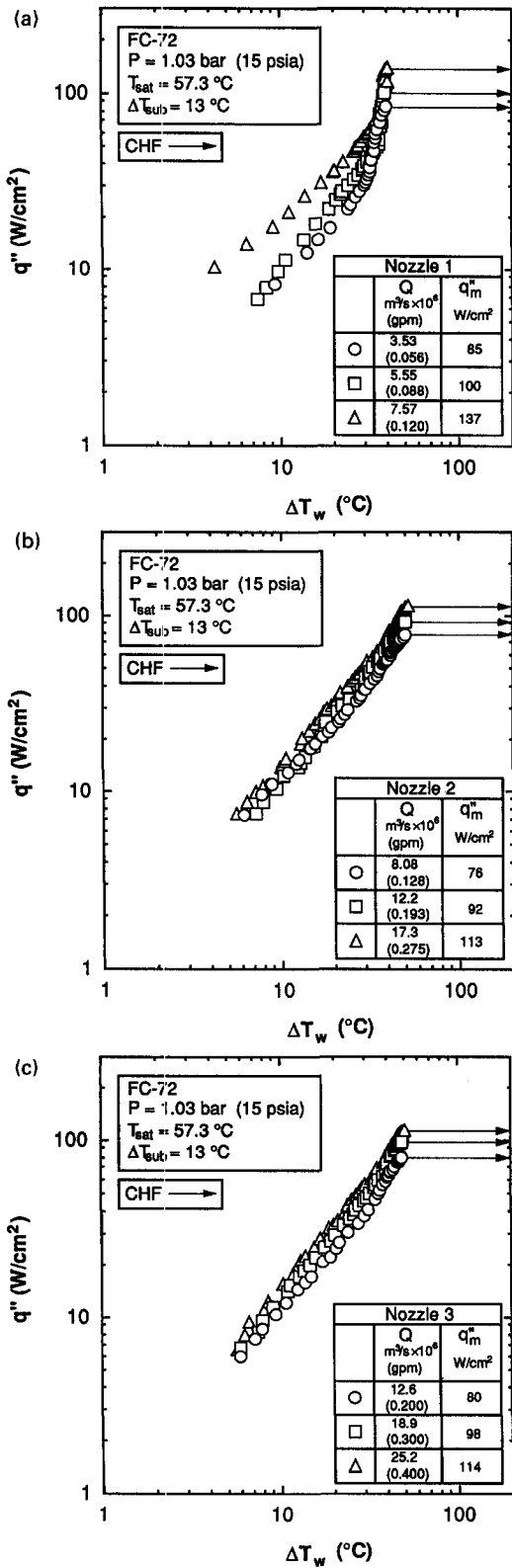| Nozzle	Orifice diameter $d_0 \times 10^6$ (m)	Spray angle θ (degrees)	Spray mean volumetric flux $\overline{Q}'' \times 10^3$ ($m^3 \ s^{-1} \ m^{-2}$)	Sauter mean diameter (SMD) $d_{32} \times 10^6$ (m)
1	762	55.8	16.6–52.4	110–196
2	1190	46.4	55.6–145	181–225
3	1700	48.5	86.3–216	182–214

Fig. 3. FC-72 boiling curves for three flow rates at 13 °C subcooling for (a) nozzle 1, (b) nozzle 2 and (c) nozzle 3.
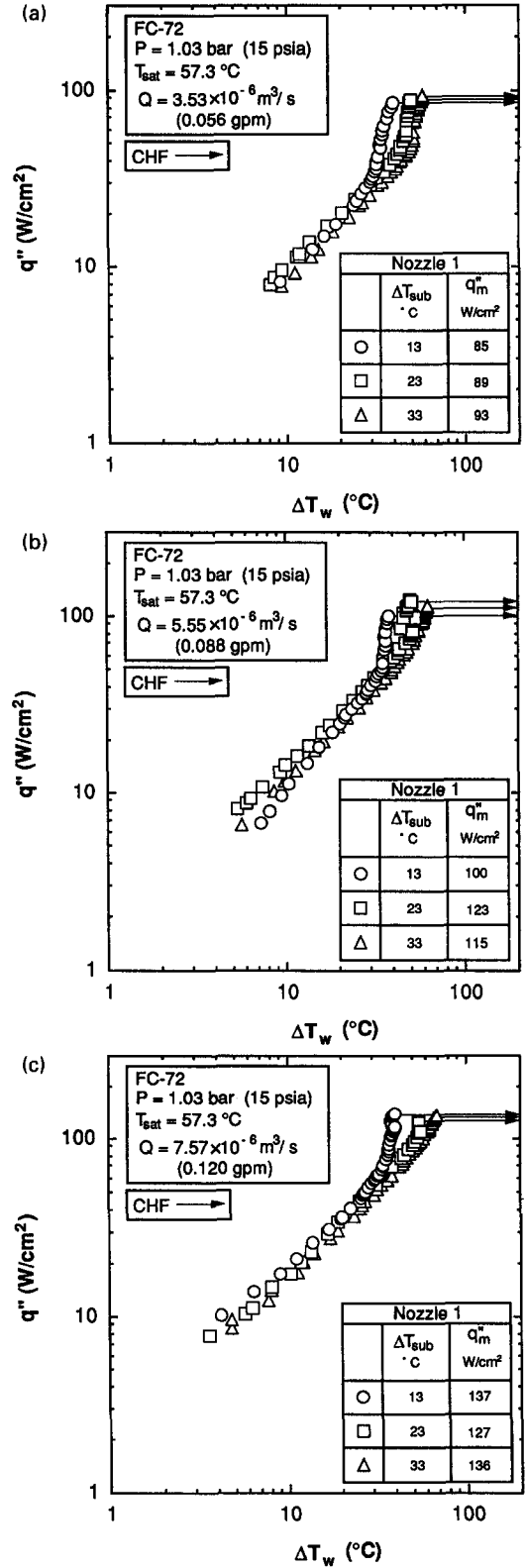
Fig. 4. FC-72 boiling curves for nozzle 1 for three subcoolings at (a) $Q = 3.53 \times 10^{-6}$ m^3 s^{-1}, (b) $Q = 5.55 \times 10^{-6}$ m^3 s^{-1} and (c) $Q = 7.57 \times 10^{-6}$ m^3 s^{-1}.
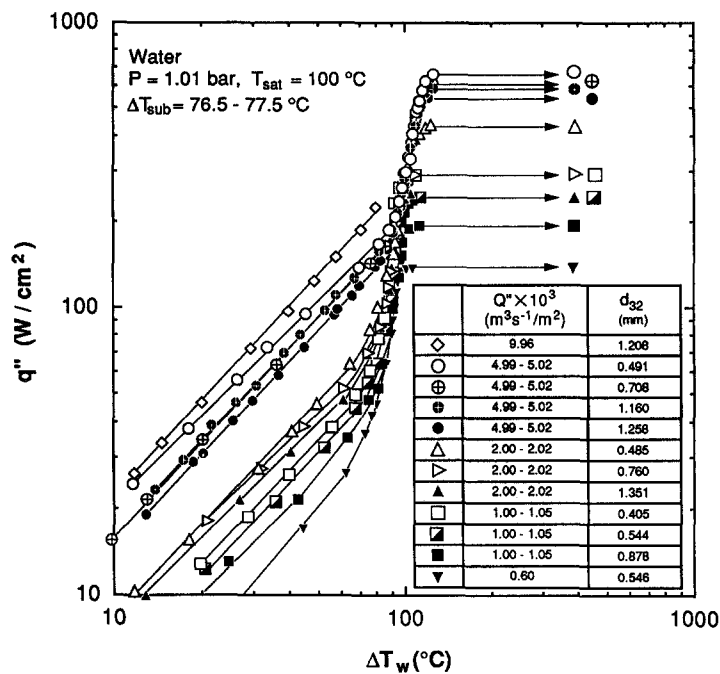
Fig. 5. Boiling curves measured by Mudawar and Valentine [2] for full cone water sprays.

of all the nucleate boiling data onto a single line, regardless of volumetric flux or drop diameter, and the relatively large slope (about 5.6) of the nucleate boiling regime. Comparing these water boiling curves to the curves for FC-72 given in Figs. 3(a)–(c) and 4(a)–(c) clearly points to the sensitivity of the slope in the nucleate boiling regime to working fluid, volumetric flux and subcooling.

Evaporation efficiency

A parameter characterizing the efficiency of liquid evaporation was employed to explain the unique shape of boiling curve described in the previous section. This efficiency was defined as the percentage of the total heat that could be removed by the spray, sensible and latent, that was actually removed at CHF

$$\eta = \frac{q''_m}{q''_{dryout}} \times 100\%$$

$$= \frac{q''_m}{\rho_f Q'' h_{fg}(1 + c_{p,f}\Delta T_{sub}/h_{fg})} \times 100\%. \quad (2)$$

Figure 6 shows efficiency vs spray Weber number for FC-72 and FC-87 at all volumetric flow rates and subcoolings and all three nozzles. Also shown are water data for full cone sprays measured by Mudawar and Valentine. Figure 6 shows that evaporation efficiency is inversely related to the Weber number, decreasing from a nearly 100% efficiency for $We < 10^{-5}$ to less than 10% for $We > 0.1$. Water tests had much smaller Weber numbers than the FC-72 and FC-87 tests, resulting in more of the liquid impinging upon the heated surface evaporating. A relatively small Weber number (water data) corresponds to a

smaller volumetric flux and, to a lesser extent, greater surface tension. A small volumetric flux reduces liquid buildup, exposing the surface to direct impingement by the drops. Evaporation of a large percentage of the spray liquid is manifest both in a larger heat flux span in the nucleate boiling regime and a large increase in slope upon transition from single-phase liquid cooling to nucleate boiling. This is illustrated clearly in Figs. 3(a)–(c) where the low flow rate, low Weber number cases exhibit a large increase in slope and the boiling curves with higher volumetric flow rates (higher Weber numbers) do not.

Using extensive high-speed photographic analysis of individual water drops impinging upon a heated surface, Bernardin [7] showed that even at surface temperatures close to CHF, boiling does not commence in the impinging liquid until the drop flattens out into a thin liquid film and loses most of its radial momentum. Thus, the early stages of drop impact during the nucleate boiling regime are dominated by single-phase heat transfer. The high, instantaneous single-phase heat transfer coefficient associated with the droplet impingement seems to suppress any nucleation. Only as the convection coefficient greatly diminishes due to loss of liquid momentum do the wall cavities acquire enough superheat to begin boiling.

This important mechanism sheds much light upon the evaporation efficiency trends revealed in Fig. 6. A spray possessing a small volumetric flux (i.e. low spray Weber number) can be classified as a light spray. Conversely, a high volumetric flux (i.e. high Weber number) spray carries the classification of dense spray. Figure 7 compares nucleate boiling with those two types of sprays. In a light spray, the frequency of drop
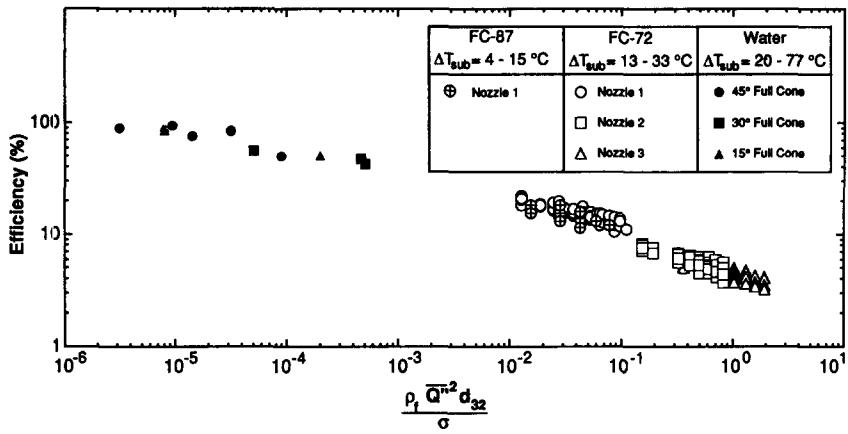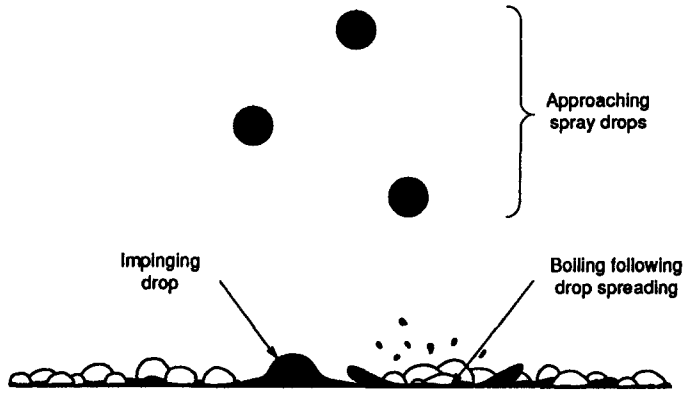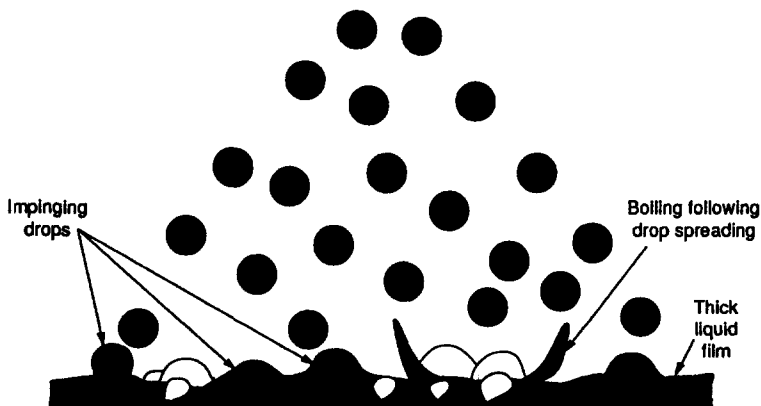
Fig. 6. Evaporation efficiency vs spray Weber number.

Light Spray: Low We, high evaporation efficiency

Dense Spray: High We, low evaporation efficiency

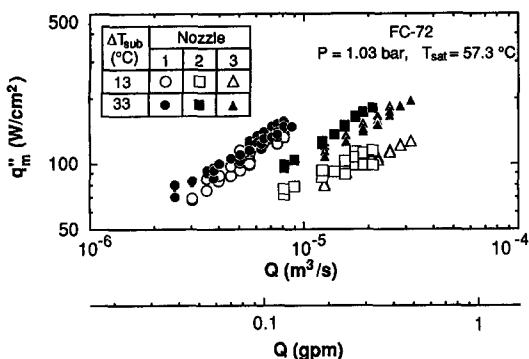Fig. 7. Schematic representation of boiling in light and dense sprays.

Fig. 8. CHF vs total volumetric flow rate for nozzles 1, 2 and 3 using FC-72.

impingement upon the heated surface is low, leaving much of the surface covered with fairly stagnant liquid within which vapor bubbles can easily nucleate. Evaporation efficiency in light sprays is, therefore, very high. Dense sprays, on the other hand, are characterized by a high frequency of droplet impingement which suppresses nucleation over a large fraction of the heated surface, resulting in a poor evaporation efficiency. This description of drop impact during nucleate boiling also explains why volumetric flux is of much greater significance to characterizing spray heat transfer than drop velocity; for, while drop velocity affects the local heat transfer from the heated surface momentarily, it is the volumetric flux that determines the commutative effect of multiple drop impingement. In fact, all attempts at correlating the present spray CHF data relative to drop velocity proved very unsuccessful.

Critical heat flux

A CHF database was collected using FC-72 for flow rates ranging from 2.52×10^{-6} to 3.15×10^{-5} m^3 s^{-1}

(0.04 to 0.5 gpm) and subcooling from 13 to 33 °C using the three spray nozzles with overlapping flow-rate ranges.

Figure 8 shows CHF values for FC-72 for all three nozzles for the high and low subcoolings; intermediate values have been left out for clarity. CHF was found to increase with increasing flow rate for each nozzle at all values of subcooling. Nozzle 1 had larger CHF values than the two larger nozzles at the same flow rate, highlighting the important effect of drop size on CHF. Smaller drops possess a greater surface area to volume ratio than do larger drops; therefore, the smaller drops can utilize their sensible and latent heat more effectively than the larger drops can. In the present study, nozzle 1 produced much smaller drops for a given flow rate than did nozzles 2 or 3. Likewise, drops of nozzle 2 were slightly smaller than those for nozzle 3 at the same flow rate, and, as indicated in Fig. 8, CHF values were greater for nozzle 2 than for nozzle 3. Figure 8 also shows CHF increased with increasing subcooling for each nozzle because of the increased amount of heat the liquid could absorb prior to evaporation.

4. SAUTER MEAN DIAMETER CORRELATION

The sprays tested in the present study were characterized by a Phase Doppler Particle Analyzer (PDPA). This non-intrusive technique enabled determination of the spray hydrodynamic parameters without disrupting the spray itself. As shown in Fig. 9, light produced by a 3 W argon-ion laser was split into two coherent beams using a beam splitter. Measurements were made at the control volume formed by intersection of the two beams. The interference fringe pattern produced by light scattered by individual drops as they passed through the control volume was captured by optical detectors. The phase difference
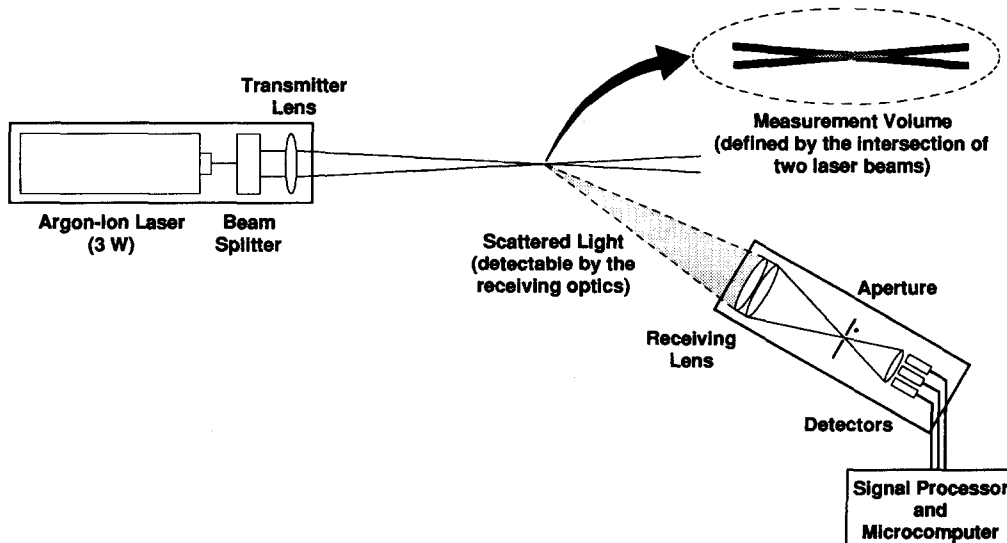

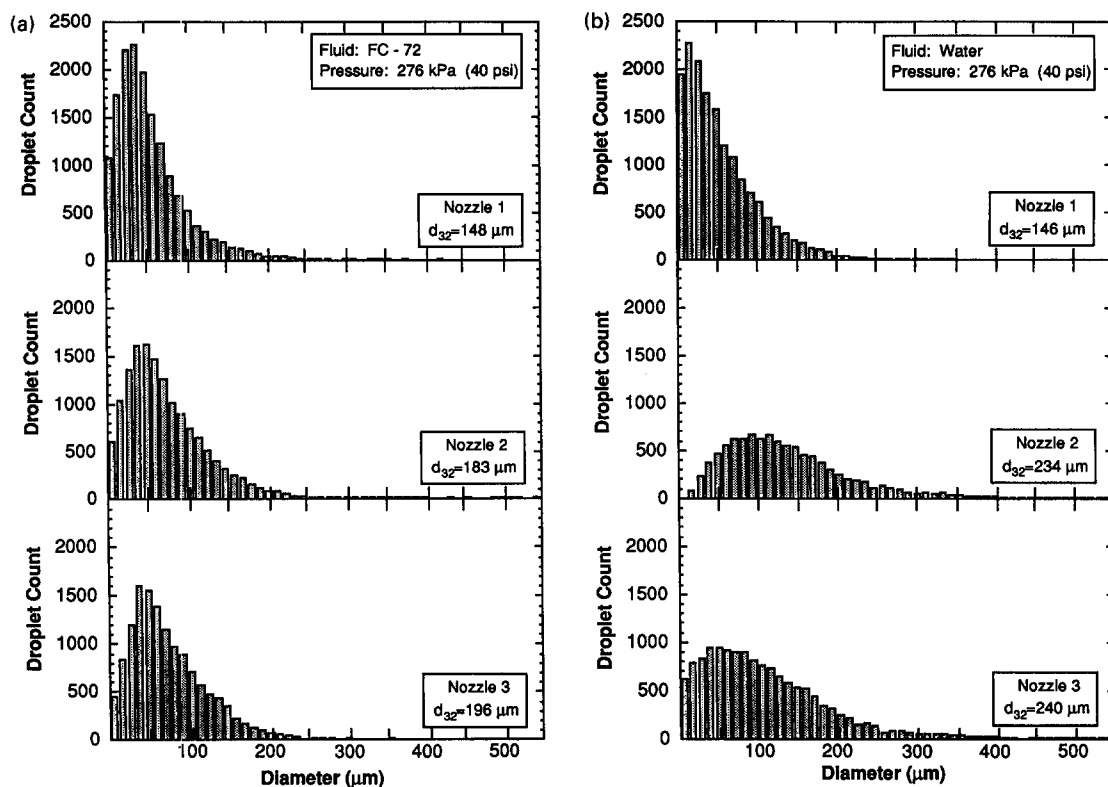Fig. 9. Phase Doppler Particle Analyzer (PDPA) optics (adapted from [8]).

Fig. 10. Drop size histograms for nozzles 1, 2 and 3 using (a) FC-72 and (b) water.

between the signals from the different detectors was proportional to the size of the drop passing through the control volume. The detector signals were processed and conditioned for data acquisition and analysis using a microcomputer.

The spray's SMD was determined along the axis of the spray for each nozzle at room temperature, $T_f = 23\,^{\circ}C$. Measurements made away from the axis proved SMD was fairly uniform. The measurements along the spray axis were taken at specific nozzle-to-surface distances and pressure drops. Drop sizes in the FC-72 sprays were measured at a distance of 45 mm from the nozzle orifice which both ensured a fully developed spray and precluded the multiple beam scattering sometimes encountered in the measurement of very dense sprays.

Figures 10(a) and (b) show, for each of the three nozzles, drop size histograms for FC-72 and water respectively, for the same pressure drop of 276 kPa (40 psi). Generally, water produced slightly larger drops than FC-72. Drop sizing was repeated for different pressure drops, and curve fits were developed to determine SMD for the pressure drop at which CHF was later measured.

A correlation for SMD would enable a designer to predict heat transfer performance of a given spray without having to perform the costly and time consuming optical drop sizing. Many correlations have been developed which predict SMD for various spray types, however, none is available for full cone sprays.

Therefore, a new correlation is developed using SMD data for the three full cone spray nozzles and two fluids: FC-72 and water.

Lefebvre [9] proposed a systematic model to describe the breakup of a sheet of liquid into spray droplets that was successful at correlating SMD data for hollow cone sprays. He suggested the breakup was caused by both aerodynamic forces downstream of the orifice as well as turbulent fluctuations in the liquid upstream of the orifice. He recommended a general correlation for dimensionless SMD, ratio of SMD to thickness of the liquid sheet, as a function of a Weber number and a Reynolds number, both based on liquid velocity and thickness of the liquid sheet.

Since full cone spray nozzles do not produce a liquid sheet prior to exiting the orifice, the characteristic length and velocity chosen for correlating SMD in the present study were the orifice diameter, d_0, and liquid velocity at the orifice, defined as $(2\Delta P/\rho_f)^{0.5}$. The Weber and Reynolds numbers based on the orifice conditions were defined, respectively, as

$$We_{d_0} = \frac{\rho_a(2\Delta P/\rho_f)d_0}{\sigma} \tag{3}$$

and

$$Re_{d_0} = \frac{\rho_f(2\Delta P/\rho_f)^{1/2}d_0}{\mu_f} \tag{4}$$

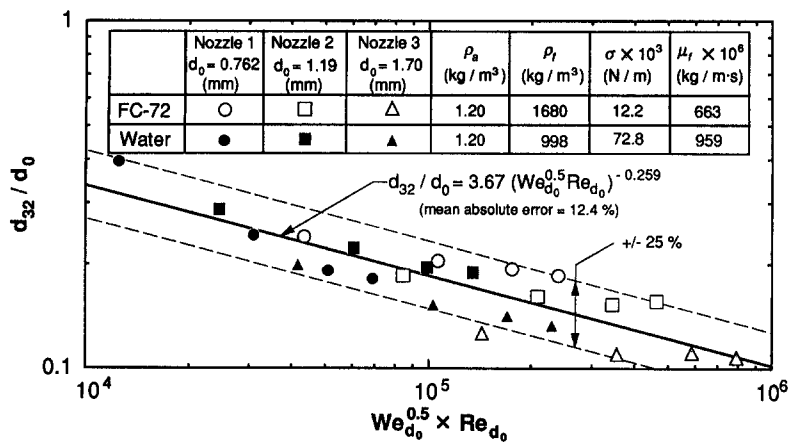where ρ_a is the density of ambient fluid (air or vapor).

Fig. 11. SMD correlation.

The resulting correlation,

$$\frac{d_{32}}{d_0} = 3.67[We_{d_0}^{1/2} Re_{d_0}]^{-0.259} \qquad (5)$$

fits the SMD data for both FC-72 and water with a mean absolute error of 12.4% as shown in Fig. 11. Interestingly, the product of the square root of Weber number and Reynolds number in equation (5) is identical in form to the product proposed by Lefebvre for hollow cone sprays.

5. CHF CORRELATION

Mudawar and Valentine [2] correlated CHF data for water using equation (1). Unlike the present Fluorinert data, their water data were measured by a circular test heater whose surface area was much smaller than the spray impact area. Essentially, both CHF and volumetric flux were measured at a single point in the water sprays; hence, the respective designations $q''_{m,p}$ and Q''. Note that, for the water data, the mean volumetric flux upon the heater's surface was equal to the local volumetric flux, $\overline{Q''} = Q''$. This water spray configuration is illustrated in Fig. 12(a), which also includes a plot showing CHF for different full cone spray nozzles increasing with increasing volumetric flux and subcooling.

The CHF correlation form proposed by Mudawar and Valentine for water data was employed to correlate the FC-72 and FC-87 CHF data obtained in the present study. Two modifications were needed to allow the Fluorinert data to be correlated with the water data using the same equation. As shown in Fig. 12(b), the Fluorinert sprays were configured so that their impact area just inscribed the heater surface following the optimization guideline developed by Estes [6]. For the Fluorinerts, critical heat flux, q''_m, was measured as the heater power divided by the total heater surface area, and the mean volumetric flux,

$\overline{Q''}$, as the total spray volumetric flow rate divided by the impact area. It is postulated that surface dryout at CHF commences at the outer edge of the impact area, where volumetric flux is a minimum, since this local dryout would reduce the fraction of the surface area available for cooling and increase the heat flux within the impact area, enabling the dryout region to propagate radially inward in an unstable manner. Therefore, CHF at the edge of the impact area should govern CHF for the entire surface. Critical heat flux at the edge was determined by assuming all of the heat was transferred through the impact area,

$$q''_{m,p} = \frac{q''_m L^2}{(\pi/4)L^2} = \frac{4}{\pi}q''_m. \qquad (6)$$

Volumetric flux at the outer edge of the impact area was determined from the spray flux distribution model developed by Estes [6]

$$\frac{Q''}{\overline{Q''}} = \frac{1}{2}[1 + \cos(\theta/2)]\cos(\theta/2). \qquad (7)$$

Figure 13 shows that the correlation

$$\frac{q''_{m,p}}{\rho_g h_{fg} Q''} = 2.3\left(\frac{\rho_f}{\rho_g}\right)^{0.3}\left(\frac{\rho_f Q''^2 d_{32}}{\sigma}\right)^{-0.35}$$
$$\times \left(1 + 0.0019\frac{\rho_f c_{p,f}\Delta T_{sub}}{\rho_g h_{fg}}\right) \qquad (8)$$

fits the CHF data for water, FC-72 and FC-87 with a mean absolute error of 12.6%. SMD for FC-87 was determined using the drop size correlation developed earlier in equation (5), as drop sizes for FC-87 were not measured. Accurate prediction of the FC-87 data is proof that CHF for full cone sprays can be predicted using equations (5) and (8) without the need for expensive drop-sizing equipment. Close inspection of equations (5) and (8) also reveals which spray parameters actually influence CHF. These parameters include thermophysical properties (ρ_f, ρ_g, σ, h_{fg}, c_{pf}),
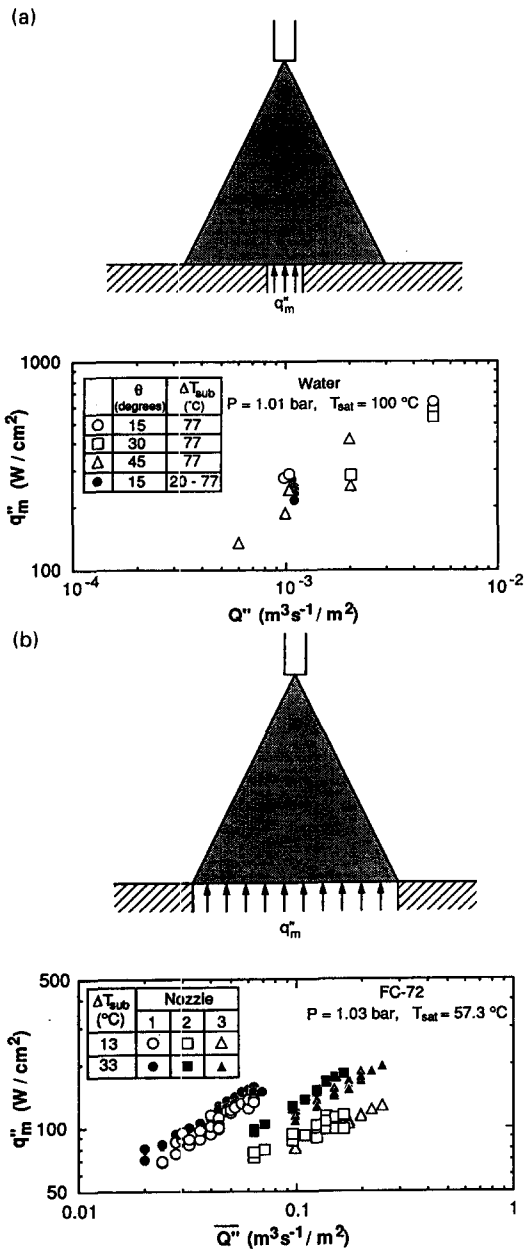
(a)

(b)

Fig. 12. (a) Mudawar and Valentine's CHF data for water [2] vs local volumetric flux and (b) present CHF data for FC-72 vs mean volumetric flux.

flow parameters (ΔT_{sub}, ΔP, Q), orifice parameters (d_0, θ), and heater length (L). The important effect of nozzle-to-surface distance (H) is implicitly a function of both heater size and spray cone angle for a spray which has been configured to optimize CHF; one whose impact area just inscribes the square heated surface.

The reader is cautioned to avoid using the present CHF correlation for sprays which are not hydrodynamically fully developed. Sprays require a minimum pressure drop and minimum nozzle-to-surface

distance to ensure complete breakup into drops. Poor breakup could greatly reduce CHF relative to predictions based upon equation (8). Some of these effects are evident in the lowest volumetric flux data in Fig. 13 for each of the nozzles used with FC-72 and FC-87. The lowest volumetric flux for each nozzle corresponds to the lowest nozzle pressure drop required for liquid breakup. These data show the largest deviation from the correlation whereas the high volumetric flux data, which correspond to large pressure drops and complete breakup, are more accurately predicted by the correlation.

6. CONCLUSIONS

Experiments were performed to understand better nucleate boiling and CHF in sprays, and to develop correlations for the spray's SMD and CHF, which would enable accurate determination of CHF for different fluids and different full cone nozzles without having to conduct expensive and laborious drop-sizing measurements. The following are the key conclusions from the study.

(1) The shape of the boiling curve of sprays is markedly different from that of other boiling systems. Sprays with high volumetric flux (high Weber number) show little increase in slope of the boiling curve between the single-phase and nucleate boiling regimes because of a suppression of nucleation and reduced evaporation efficiency. Low volumetric flux (low Weber number) sprays, on the other hand, display a more pronounced increase in the slope of the boiling curve because of a higher evaporation efficiency.

(2) CHF increases with increasing flow rate and increasing subcooling; CHF is also greater for nozzles which produce smaller drops.

(3) SMD for full cone sprays is dependent upon orifice diameter and the Weber and Reynolds numbers based on the orifice flow conditions prior to liquid breakup. A dimensionless correlation was developed which gives good predictions for fluids with vastly different surface tensions.

(4) A correlation was developed which accurately predicts CHF for water, FC-72 and FC-87 and many different full cone nozzles over a wide range of flow rates and subcoolings. This correlation demonstrates that CHF is influenced by the thermophysical properties of the fluid (ρ_f, ρ_g, σ, h_{fg}, $c_{p,f}$), flow parameters (ΔT_{sub}, ΔP, Q), orifice parameters (d_0, θ), and heater length (L).

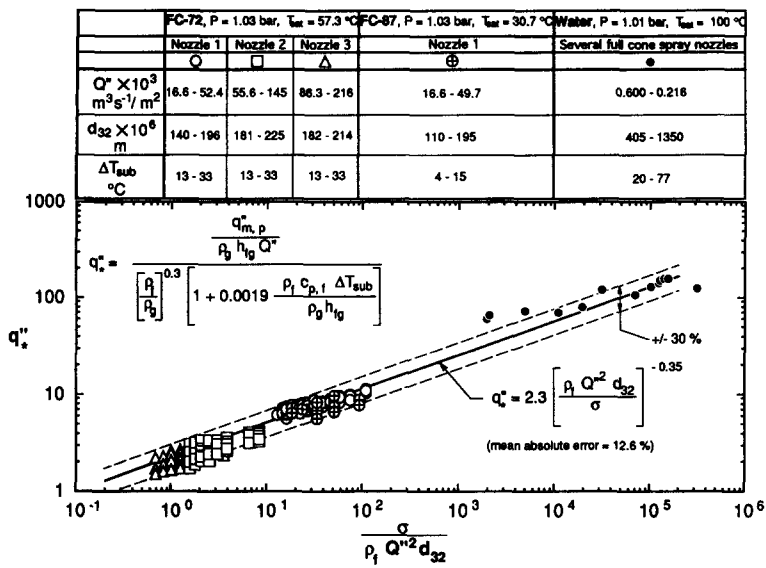|	FC-72, P = 1.03 bar, T_{sat} = 57.3 °C			FC-87, P = 1.03 bar, T_{sat} = 30.7 °C	Water, P = 1.01 bar, T_{sat} = 100 °C
	Nozzle 1	Nozzle 2	Nozzle 3	Nozzle 1	Several full cone spray nozzles
	O	□	△	⊕	●
$Q'' \times 10^3$ $m^3 s^{-1}/m^2$	16.6 - 52.4	55.6 - 145	86.3 - 216	16.6 - 49.7	0.600 - 0.216
$d_{32} \times 10^6$ m	140 - 196	181 - 225	182 - 214	110 - 195	405 - 1350
ΔT_{sub} °C	13 - 33	13 - 33	13 - 33	4 - 15	20 - 77

Fig. 13. CHF correlation.

REFERENCES

1. S. Toda, A study in mist cooling, *Trans. JSME* **38**, 581–588 (1972).
2. I. Mudawar and W. S. Valentine, Determination of the local quench curve for spray-cooled metallic surfaces, *J. Heat Treating* **7**, 107–121 (1989).
3. G. E. Totten, C. E. Bates and N. A. Clinton, *Handbook of Quenchants and Quenching Technology*, pp. 239–289. ASM International, Materials Park, OH (1993).
4. I. Mudawar T. A. and Deiters, A universal approach to predicting temperature response of metallic parts to spray quenching, *Int. J. Heat Mass Transfer* **37**, 347–362 (1994).
5. C. S. K. Cho and K. Wu, Comparison of burnout characteristics in jet impingement cooling and spray cooling, *Proc. National Heat Transfer Conf.*, pp. 561–567. Houston, TX (1988).

6. Estes, K. A., Critical heat flux in spray cooling and jet impingement cooling of small targets, Masters Thesis, School of Mechanical Engineering, Purdue University, West Lafayette, IN (1994).
7. Bernardin, J. D., Intelligent heat treatment of aluminum alloys: material, surface roughness, and droplet-surface interaction characteristics, Masters Thesis, School of Mechanical Engineering, Purdue University, West Lafayette, IN (1993).
8. D. D. Hall, A method of predicting and optimizing the thermal history and resulting mechanical properties of aluminum alloy parts subjected to spray quenching, Masters Thesis, School of Mechanical Engineering, Purdue University, West Lafayette, IN (1993).
9. A. H. Lefebvre, *Atomization and Sprays*, Hemisphere Publishing Corporation, New York, NY (1989).